Coexisting Hidden Attractors in a 4-D Simplified Lorenz System

Chunbiao Li

School of Information Science and Engineering,
Southeast University, Nanjing 210096, P. R. China

Engineering Technology Research and Development
Center of Jiangsu Circulation Modernization Sensor Network,
Jiangsu Institute of Commerce, Nanjing 210007, P. R. China

Department of Physics, University of Wisconsin–Madison,
Madison, WI 53706, USA
chunbiaolee@gmail.com

J. C. Sprott

Department of Physics, University of Wisconsin–Madison,
Madison, WI 53706, USA
sprott@physics.wisc.edu

A new simple four-dimensional equilibrium-free autonomous ODE system is described. The system has seven terms, two quadratic nonlinearities, and only two parameters. Its Jacobian matrix everywhere has rank less than 4. It is hyperchaotic in some regions of parameter space, while in other regions it has an attracting torus that coexists with either a symmetric pair of strange attractors or with a symmetric pair of limit cycles whose basin boundaries have an intricate fractal structure. In other regions of parameter space, it has three coexisting limit cycles and Arnold tongues. Since there are no equilibria, all the attractors are hidden. This combination of features has not been previously reported in any other system, especially one as simple as this.

Keywords: Hidden attractors; hyperchaos; attracting torus; multistability.

1. Introduction

There has been recent interest in systems with coexisting attractors, some of which are hidden [Leonov & Kuznetsov, 2013] in the sense that they are not associated with an unstable equilibrium and thus often go undiscovered because they may occur in a small region of parameter space and with a small basin of attraction in the space of initial conditions. However, they are of considerable importance in engineering applications since they can lead to unexpected and even catastrophic behavior in a system designed to produce a particular dynamic such as the Millennium Bridge in London or the Tacoma Narrows Bridge in the State of Washington.

Similarly, after the first hyperchaotic attractor was discovered by Rössler [1979], hyperchaos has continued to attract much interest. Recently many hyperchaotic systems with specific properties have been proposed. For example, Wang *et al.* [2012] proposed a hyperchaotic system without any equilibrium. Qi *et al.* [2008] proposed a hyperchaotic

system with two large positive Lyapunov exponents. Chlouverakis and Sprott [2006] proposed what may be the algebraically simplest hyperchaotic snap system. Many hyperchaotic systems based on an extension of the famous Lorenz [1963] system have been proposed [Li *et al.*, 2005; Gao *et al.*, 2007; Ruy, 2007; Si *et al.*, 2011; Wang *et al.*, 2010]. However, these Lorenz-like systems have more than seven terms and more than two parameters, and thus it is difficult to characterize their dynamics completely. Except for the hyperchaotic Rössler system with a single quadratic nonlinearity but with nine terms and four parameters, other hyperchaotic systems usually have two or more nonlinearities or nonlinearities other than quadratic, and thus they lack simplicity.

In this paper, we propose a new autonomous four-dimensional system based on an extension of the diffusionless Lorenz system [van der Schrier & Maas, 2000], which is simpler than but has some similarities to the sinusoidally-forced Lorenz systems that have been previously studied [Mirus & Sprott, 1999; Li *et al.*, 2005]. It is an especially elegant system with many interesting properties not found in this combination in other proposed systems: (i) It has only seven terms, two quadratic nonlinearities, and two parameters. (ii) It has no equilibrium points and thus all attractors are hidden. (iii) It exhibits hyperchaos over a large region of parameter space. (iv) Its Jacobian matrix has rank less than 4 everywhere in the space of the parameters and dynamical variables despite the fact that the system is four-dimensional. (v) It exhibits a quasiperiodic route to chaos with an attracting torus for some choice of parameters. (vi) It has regions in which the torus coexists with either a symmetric pair of strange attractors or a symmetric pair of limit cycles and other regions where three limit cycles coexist. (vii) The basins of attraction have an intricate fractal structure. (viii) There is a series of Arnold tongues [Paar & Pavin, 1998] within the quasi-periodic region where the two fundamental oscillations mode-lock and form limit cycles of various periodicities.

In Sec. 2, we describe the system and its basic properties. In Sec. 3, we show the hyperchaotic attractor. In Sec. 4, we map out the dynamic regions in the two-dimensional parameter space. In Sec. 5, we show examples of the coexisting attractors and their fractal basins. The last section contains discussion and conclusions.

2. Proposed System and Its Properties

Among the many modified versions of the Lorenz system, probably the simplest is the diffusionless Lorenz system [van der Schrier & Maas, 2000; Munmuangsaen & Srisuchinwong, 2009], obtained by taking the limit r, $\sigma \to \infty$ but in such a way that $a = br/\sigma^2$ remains finite. The resulting five-term system has most of the properties of the classic Lorenz system but with only a single parameter a. Perhaps the simplest four-dimensional extension of this system uses linear feedback control to generate hyperchaos [Gao & Zhang, 2011], resulting in

$$
\begin{cases}
\dot{x} = y - x, \\
\dot{y} = -xz + u, \\
\dot{z} = xy - a, \\
\dot{u} = -by.
\end{cases}
\tag{1}
$$

Since the coefficients of five of the seven terms can be normalized to ± 1 through a linear rescaling of the four variables and time without loss of generality, system (1) is completely described by only two independent parameters, taken here as a and b, and thus it is possible to characterize the dynamics completely. Like the ordinary Lorenz system, system (1) has rotational symmetry with respect to the z-axis as evidenced by its invariance under the coordinate transformation, $(x, y, z, u) \to (-x, -y, z, -u)$.

The rate of hypervolume contraction is given by the Lie derivative,

$$
\nabla V = \frac{\partial \dot{x}}{\partial x} + \frac{\partial \dot{y}}{\partial y} + \frac{\partial \dot{z}}{\partial z} + \frac{\partial \dot{u}}{\partial u} = -1.
$$

Thus system (1) is dissipative with solutions as time goes to infinity that contract onto an attractor of zero measure in 4-D state space.

From the steady-state equations,

$$
\begin{cases}
y - x = 0, \\
-xz + u = 0, \\
xy - a = 0, \\
-by = 0,
\end{cases}
\tag{2}
$$

it is found that Eq. (2) has no real solutions and thus no equilibrium points when a and b are nonzero. Therefore, any attractors of the system are hidden. Furthermore, the terms on the left-hand side of Eq. (2) must time-average to zero for the attractors to be bounded.

To understand the physical meaning of the parameters a and b, linearly rescale system (1) according to $x \to \sqrt{a}x$, $y \to \sqrt{a}y$, $z \to az$, and $u \to \sqrt{a}u$ to obtain

$$\begin{cases} \dot{x} = y - x, \\ \dot{y} = -axz + u, \\ \dot{z} = xy - 1, \\ \dot{u} = -by. \end{cases} \tag{3}$$

In the limit $a \to 0$, the system separates into a 2-D linear oscillator (y–u) and a 2-D linear response system (x–z) in which y can be considered as a time-varying parameter. The amplitude of the oscillation is determined by the initial conditions, and hence there is no attractor. The parameter b is the square of the oscillation frequency, and a is a measure of the coupling of the response system back to the oscillator as well as the nonlinearity that gives rise to a second-order chaotic oscillation. These two oscillations give rise to the quasi-periodicity that occurs over much of the parameter space as well as Arnold tongues where the two systems mode-lock.

3. Hyperchaos and Dimensionality

An important feature of the system is the existence of hyperchaos for a range of parameters. The degree of hyperchaos can be quantified by the value of the second Lyapunov exponent normalized to the most negative exponent. By this criterion,

the maximum hyperchaos occurs for $a = 2.6$ and $b = 0.44$ where the Lyapunov exponents are (0.0704, 0.0128, 0, −1.0832), the Kaplan–Yorke dimension is $D_{KY} = 3.0768$ using the method of Wolf *et al.* [1985], and the correlation dimension [Sprott & Rowlands, 2001] is approximately 2.8. The projections of the hyperchaotic attractor onto various planes are shown in Fig. 1.

A counter-intuitive feature is that the Kaplan–Yorke dimension is relatively small when the hyperchaos is large, whereas the maximum Kaplan–Yorke dimension occurs for $a = 3.4693$, $b = 0$ where the system becomes three-dimensional with an extraneous $\dot{u} = 0$ equation and a constant u given by the initial condition u_0. For these conditions, the Lyapunov exponents are (0.3079, 0, 0, −1.3079), and the corresponding Kaplan–Yorke dimension $D_{KY} = 3.2354$ [Sprott, 2007].

A very unusual feature of this system is that the Jacobian matrix given by

$$J = \begin{pmatrix} -1 & 1 & 0 & 0 \\ -z & 0 & -x & 1 \\ y & x & 0 & 0 \\ 0 & -b & 0 & 0 \end{pmatrix} \tag{4}$$

has less than full rank everywhere as evidenced by the fact that the last two columns are proportional. Normally a matrix with less than full rank would suggest that there is an extraneous equation related to the others through some transformation. Yet the
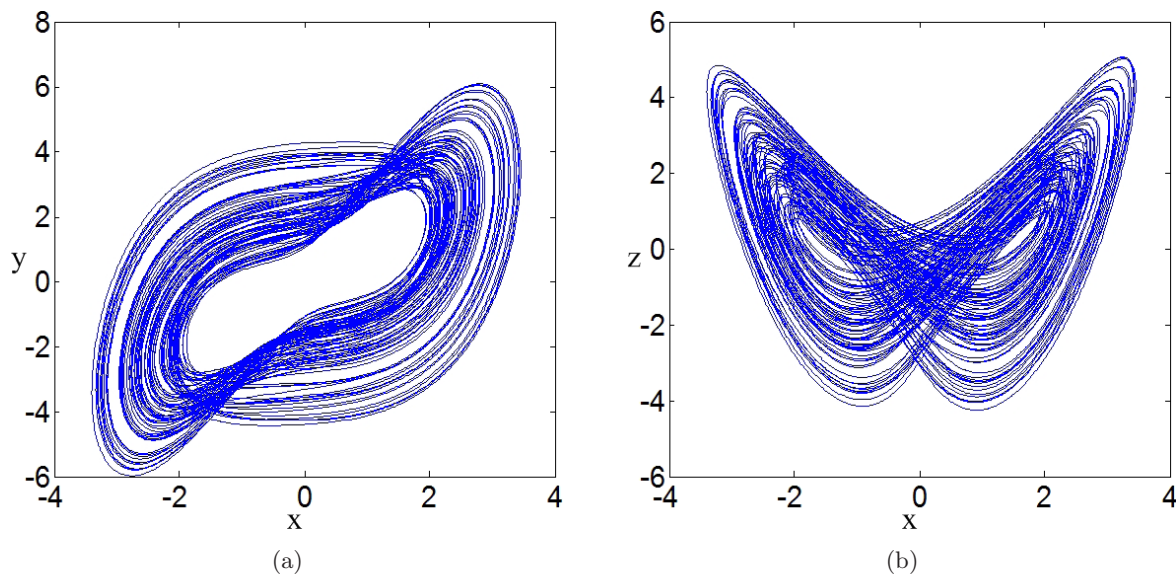

Fig. 1. Hyperchaotic attractor for system (1) with $a = 2.6$, $b = 0.44$ and initial conditions $(2, 4, 0, 0)$, (a) x–y plane, (b) x–z plane, (c) y–z plane and (d) u–x plane.
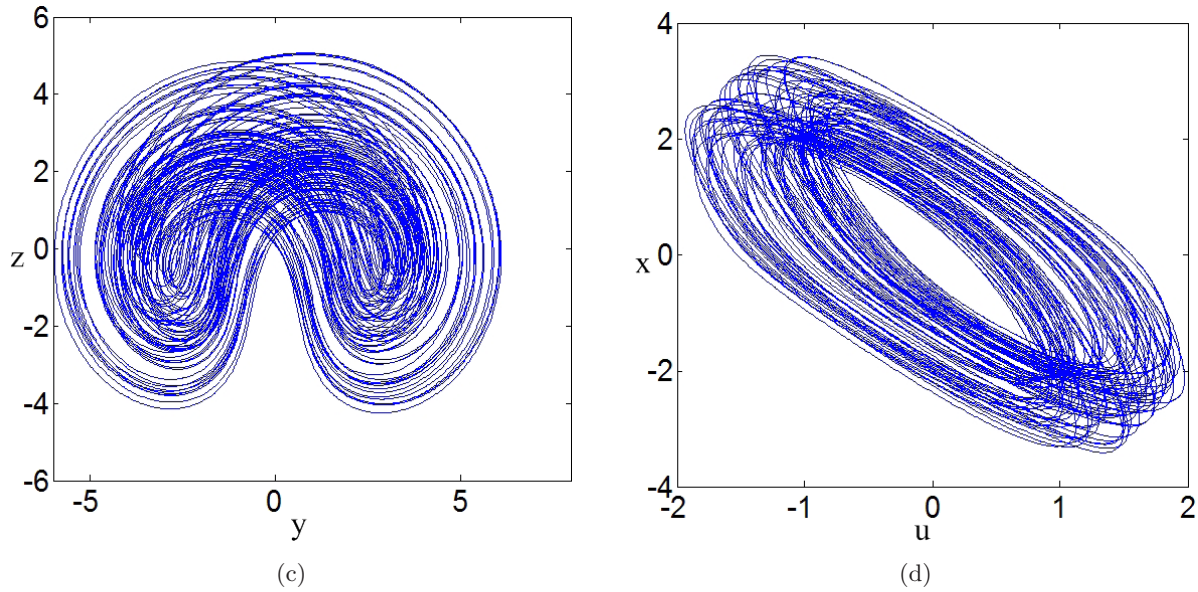
(c)

(d)

Fig. 1.   (*Continued*)

system is clearly four-dimensional because it has four distinct Lyapunov exponents and a Poincaré section in the hyperchaotic region whose dimension is at least 2.0 as shown in Fig. 2. To our knowledge, no other chaotic system with this property has been reported.
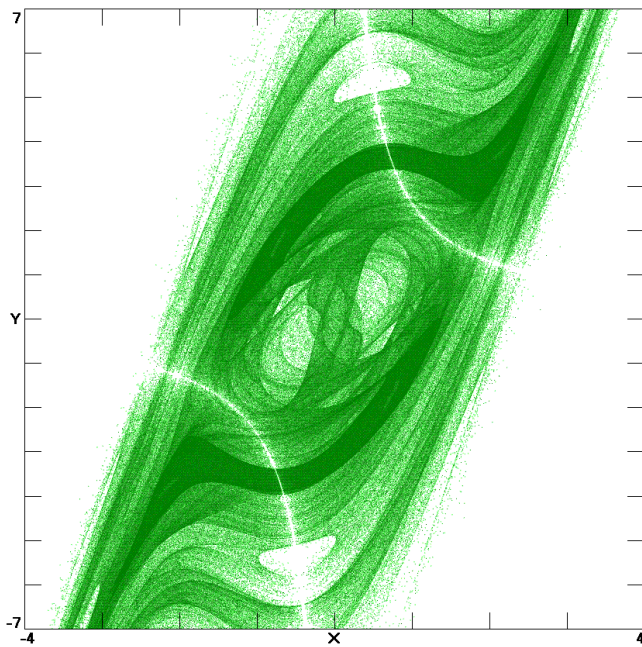
4. Dynamical Regions

The different dynamical regions in the space of the parameters a and b as determined from the Lyapunov exponent spectra are shown in Fig. 3. For this plot, initial conditions were chosen randomly from
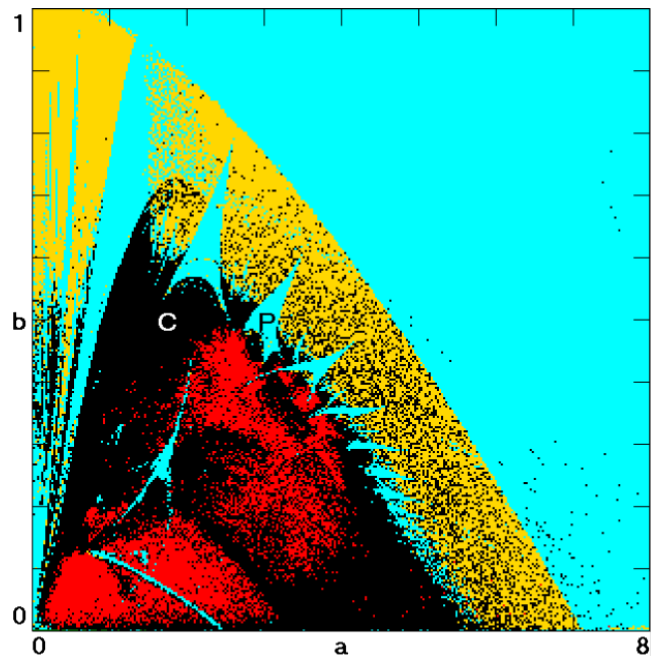

Fig. 2.   Projection onto the x–y plane of a cross-section of the attractor at $z = 0$ for system (1) with $a = 2.6$, $b = 0.44$ and initial conditions (2, 4, 0, 0). The white lines are hyperbola with $xy = a$ where $\dot{z} = 0$.

Fig. 3.   Regions of various dynamical behaviors as a function of the bifurcation parameters a and b. The hyperchaotic regions are shown in red, the chaotic regions are shown in black, the quasi-periodic regions are shown in yellow, and the periodic regions are shown in blue.
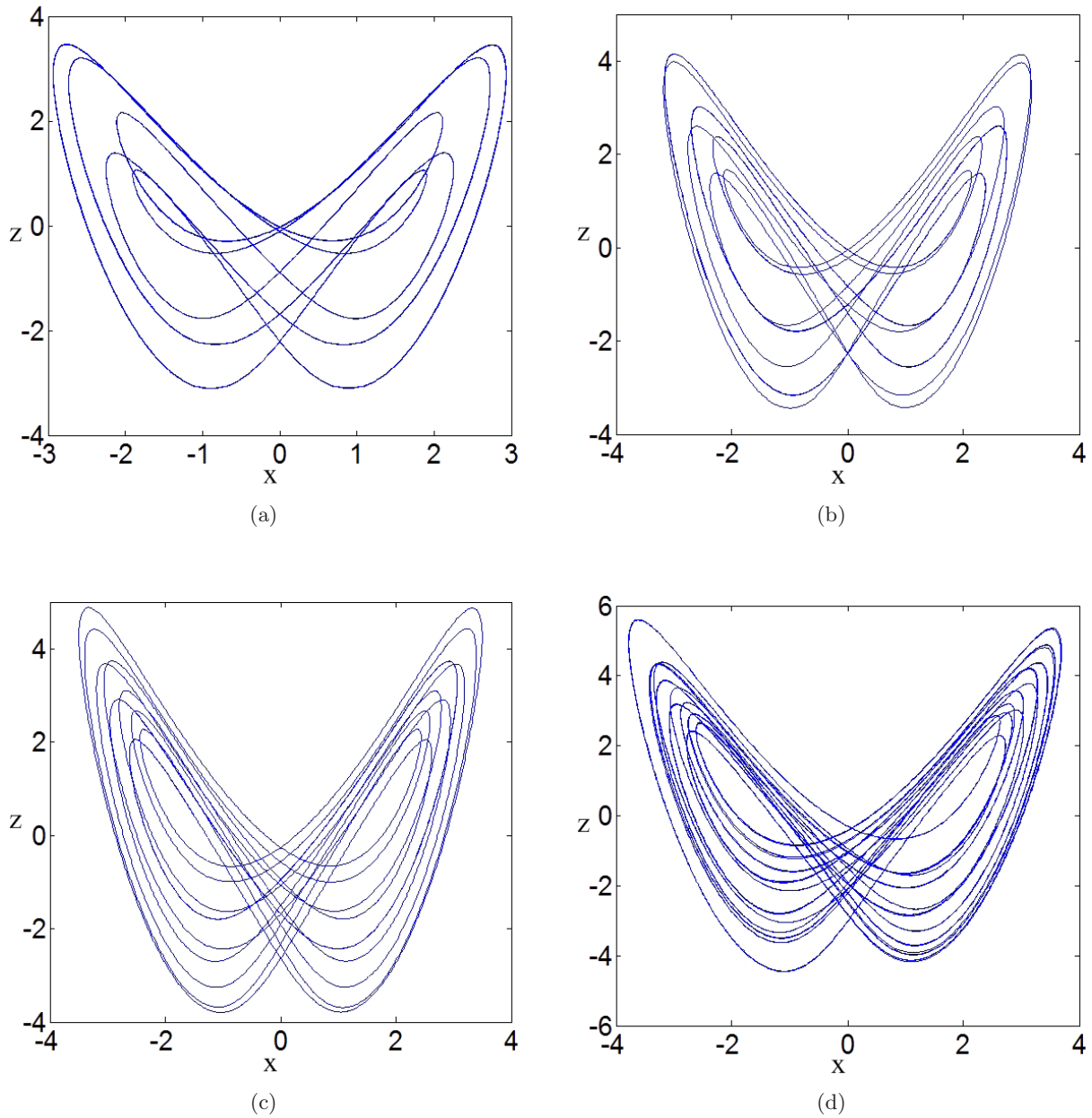
Fig. 4. Projection onto the x–z plane of limit cycles within the Arnold tongues for initial conditions $(1, -1, 1, -1)$, (a) 5-cycle at $a = 2.4$ and $b = 0.6$ with LEs $(0, -0.0116, -0.0481, -0.9403)$, (b) 7-cycle at $a = 2.9$ and $b = 0.48$ with LEs $(0, -0.0085, -0.0149, -0.9766)$, (c) 9-cycle at $a = 3.5$ and $b = 0.42$ with LEs $(0, -0.0071, -0.0071, -0.9858)$ and (d) 11-cycle at $a = 3.9$ and $b = 0.36$ with LEs $(0, -0.0011, -0.0131, -0.9859)$.

a Gaussian distribution of mean zero and variance one for each of the 800×800 pixels in the plot. Thus the dotted regions suggest the possibility of coexisting attractors of different types but could also represent long-duration transients.

As shown in the figure, system (1) has four main dynamical regions depending on the parameters a and b with a number of important properties:

(1) Because system (1) has no equilibrium points, the limit cycle is the main rhythm of solution. Different limit cycles exist both at large a and in a window between the torus and the chaotic region dominated by Arnold tongues, as well as in windows amidst the chaos and in the region with coexisting attractors. The absence of any equilibrium means that system (1) could be used as the basis for a periodic oscillator with no danger that the oscillations would stop. Some typical symmetric limit cycles in the Arnold tongues are shown in Fig. 4. In other regions, a symmetric limit cycle coexists with a symmetric pair of limit cycles for different initial conditions as shown in Fig. 5. All these limit cycles are different, which shows that the system has abundant periodic oscillations for different parameter combinations.

(2) Like other coupled oscillators, the oscillation frequency in this system has different values in the different tongues where mode-locking occurs, and in fact within the tongues are multiple coexisting limit cycles and bifurcations where the period changes abruptly.

(3) Besides limit cycles, system (1) has quasi-periodicity, chaos, and hyperchaos, which can make control difficult in practical applications where a particular dynamic is desired.

(4) System (1) has regions of parameter space where there are different attracting toruses as shown in Fig. 6. From Fig. 3, we see that the system exhibits a quasi-periodic route to chaos as a decreases at a fixed small value of b. The torus forms at a secondary Hopf bifurcation with a well-defined, smooth boundary, after which the torus either develops kinks [Ruelle & Takens, 1971; Newhouse *et al.*, 1971] or the frequencies lock before becoming chaotic.

(5) The dotted dynamical regions generally indicate coexisting attractors of different types. There are regions in which a torus coexists with two limit cycles or with two strange attractors, and other regions where a limit cycle coexists with two strange attractors, examples of which will be shown shortly. The density of the dots provides some indication of the size of the basin of attraction. However, despite the dots within the red/black region, it does not appear that there are regions where hyperchaotic attractors coexist with chaotic or other
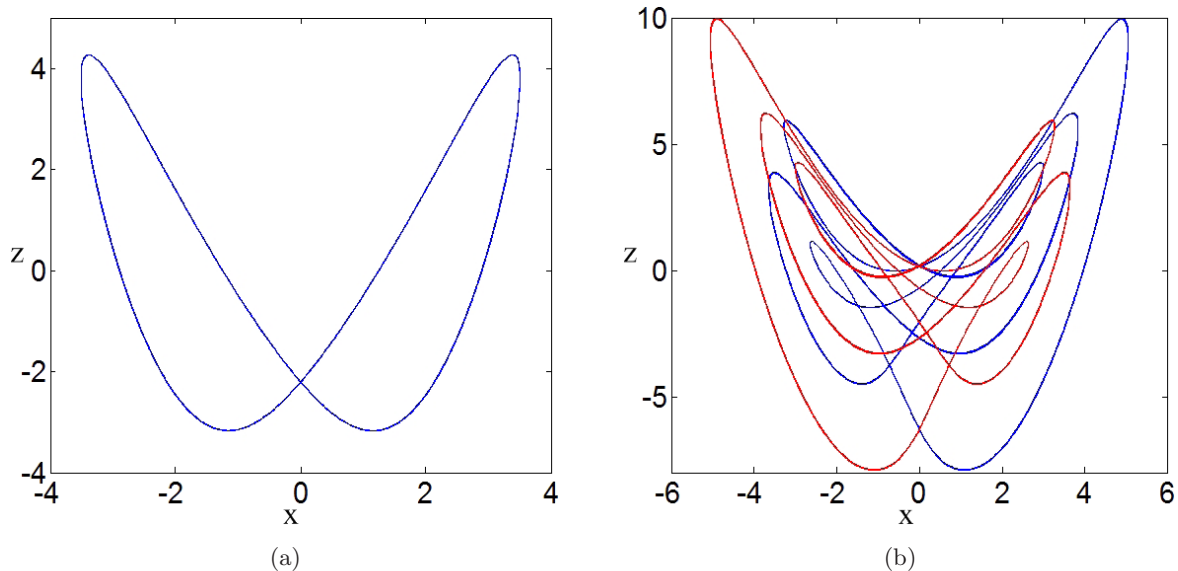

Fig. 5. Projection onto the x–z plane of the trajectory (red and blue attractors correspond to two symmetric initial conditions) with $a = 5$, $b = 0.5$. A symmetric pair of limit cycles coexists with another symmetric limit cycle. (a) Initial conditions $(0, -1, 1, -1)$ with LEs $(0, -0.0180, -0.0180, -0.9639)$ and (b) initial conditions $(\pm 0.2, \pm 5.3, 0, \pm 2)$ with LEs $(0, -0.0520, -0.0589, -0.8891)$.
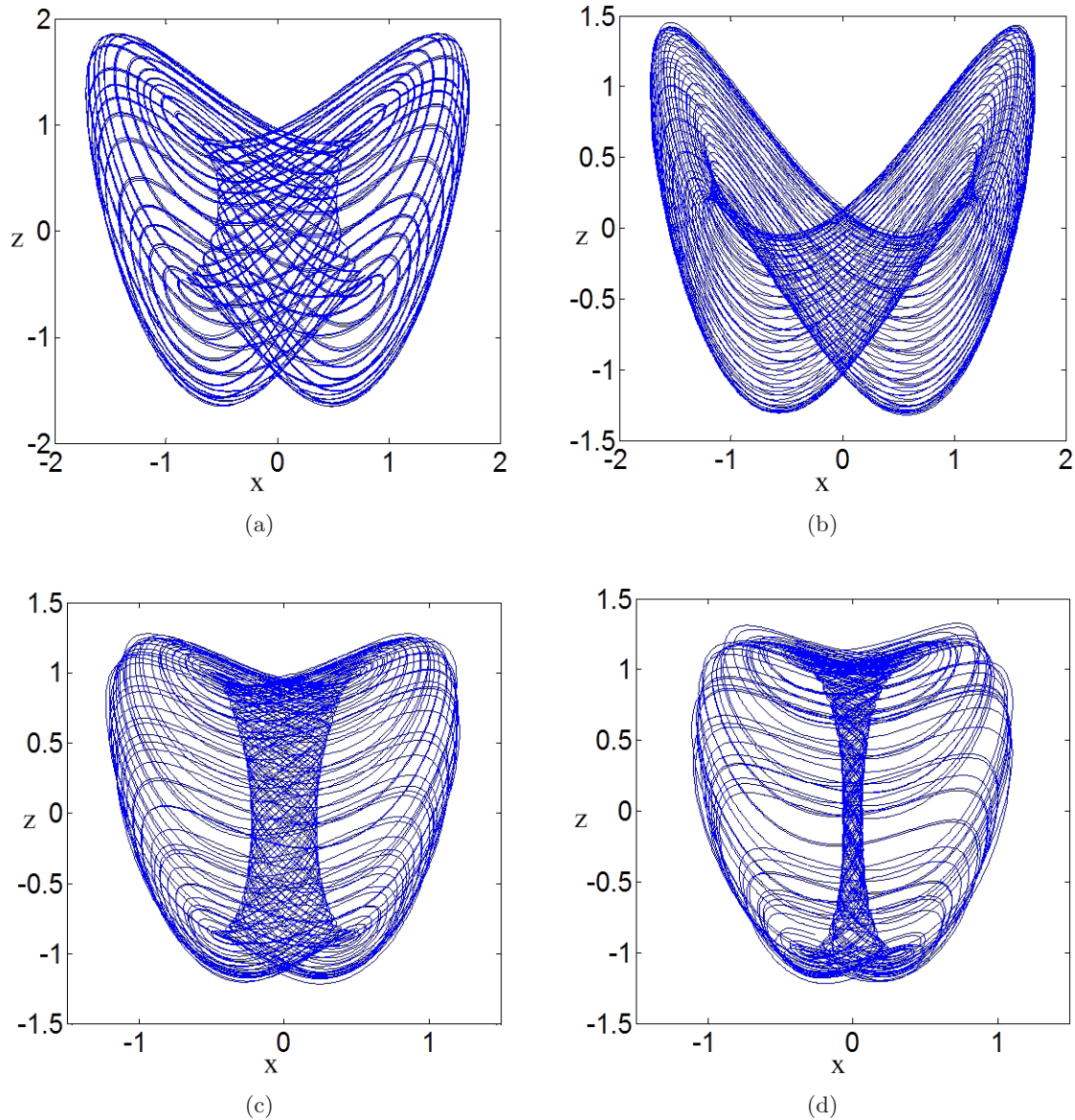
Fig. 6. Projection on the x–z plane of toruses for initial conditions $(1, -1, 1, -1)$, (a) $a = 0.6$, $b = 0.6$ with LEs $(0, 0, -0.1091, -0.8909)$, (b) $a = 1$, $b = 0.9$ with LEs $(0, 0, -0.0158, -0.9842)$, (c) $a = 0.2$, $b = 0.8$ with LEs $(0, 0, -0.0074, -0.9926)$ and (d) $a = 0.1$, $b = 0.8$ with LEs $(0, 0, -0.0034, -0.9966)$.

attractors. Rather, the boundary between chaos and hyperchaos is a fuzzy one where it is difficult to determine numerically with confidence which of the two small Lyapunov exponents is actually zero. No special bifurcation seems to be associated with this transition.

5. Coexisting Attractors

In addition to the three coexisting limit cycles shown in Fig. 5, there are three other regions where three attractors coexist. Symmetric pairs of attractors are most easily detected by calculating

the average value of the variable u since it is not constrained to be zero by the dynamical equations and in many cases is dominated by low frequency variations. Figure 7 shows a case in which an attracting torus coexists with a symmetric pair of limit cycles. In such a case, it is interesting to examine the basins of attraction of the different attracting sets, defined as the set of initial conditions whose trajectories converge on the given attractor. The boundary separating the basins can be smooth or fractal. However, the basins in this case are four-dimensional regions and have to be plotted in a two-dimensional cross-section. For $a = 2$, $b = 0.8$ where
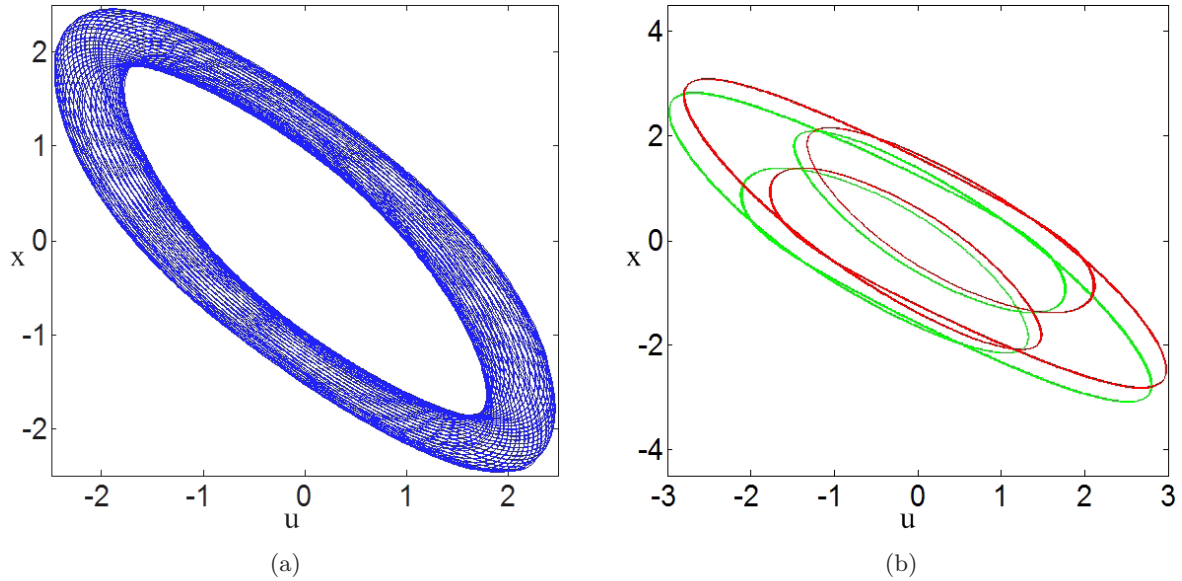
(a)　　　　　　　　　　　　　　　(b)

Fig. 7.　Torus coexisting with two limit cycles at $a = 2$, $b = 0.8$ (green and red attractors correspond to two symmetric initial conditions). (a) Initial conditions $(4, -1, 1, -1)$ with LEs $(0, 0, -0.0400, -0.9600)$ and (b) initial conditions $(\mp 5, \mp 1, 1, \mp 1)$ with LEs $(0, -0.0381, -0.1615, -0.8004)$.

a torus coexists with a symmetric pair of limit cycles in Fig. 7, the basins in the $y = 0$, $u = 0$ plane are shown in Fig. 8. The basins of the two limit cycles are indicated by red and green, respectively, and the basin of the torus is shown in blue. The basins

have the expected symmetry about the z-axis and an intricate fractal boundary.

An unusual feature of system (1) is that a symmetric pair of strange attractors coexists with an attracting torus over a relatively large region of
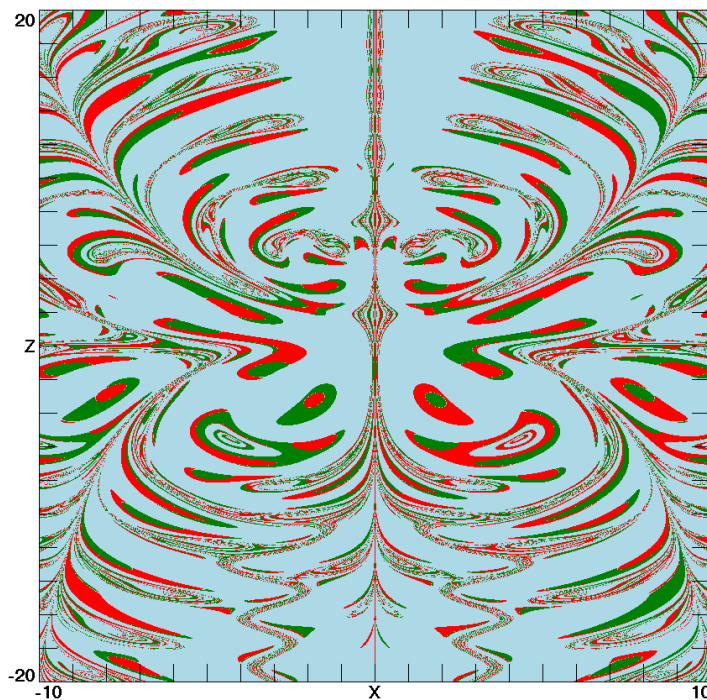

Fig. 8.　Cross-section for $y = 0$ and $u = 0$ of the basins of attraction for the torus (blue) and the symmetric pair of limit cycles (red and green) for system (1) at $a = 2$, $b = 0.8$.
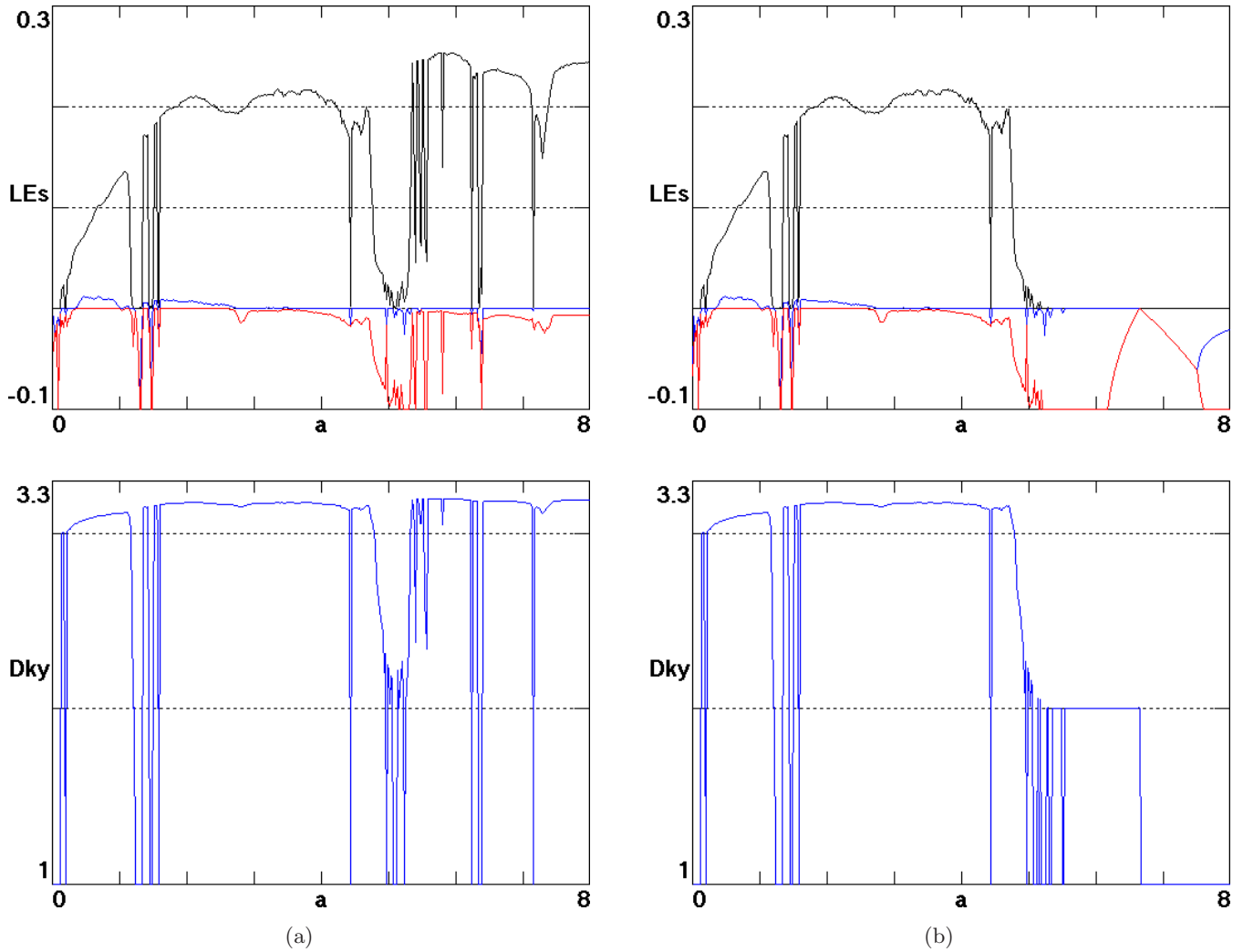
Fig. 9.   Largest three Lyapunov exponents of system (1) with $b = 0.1$ at initial conditions $(1, -1, 1, -1)$ versus a and their respective Kaplan–Yorke dimensions, (a) increasing a and (b) decreasing a.

parameter space as shown by the yellow/black dotted region in Fig. 2. Figure 9 shows the Lyapunov exponent spectra for increasing and decreasing a in the range $[0, 8]$ with $b = 0.1$. The figure indicates the range of the parameter a for which strange attractors coexist with an attracting torus or a limit cycle, most easily seen in the values of the Kaplan–Yorke dimensions. Also evident is the secondary Hopf bifurcation at $a \approx 6.7$ where the limit cycle loses its stability and the torus is born. The three attractors for $a = 6$ are shown in Fig. 10, in which the two strange attractors are interlinked in the three-dimensional xyz space but are separated in u. The basins of attraction are shown in Fig. 11 with the symmetric pair of strange attractors indicated by red and green, respectively, and the basin of the torus is in blue. The basins resemble those in Fig. 8 with symmetry and intricate fractal boundaries.

Figure 9 shows a region in the vicinity of $a = 5$ with $b = 0.1$ that is rich in bifurcations. With decreasing a, the torus becomes unstable at $a \approx 5.078$, whereupon a symmetric strange attractor is born. The trajectory on this attractor slowly drifts back and forth in the u-direction, while the dynamics are fast in the other dimensions. At about the same value of a, the symmetric pair of strange attractors is destroyed in a boundary crisis. In addition, there are long-duration transients in this region. Figure 9 also shows another example of the hyperchaotic region not coinciding with the region of largest Kaplan–Yorke dimension.

Moreover, for large values of a and small values of b, a limit cycle coexists with a symmetric pair of strange attractors whose trajectories for $a = 7$ and $b = 0.1$ are shown in Fig. 12 with basins of attraction as shown in Fig. 13.

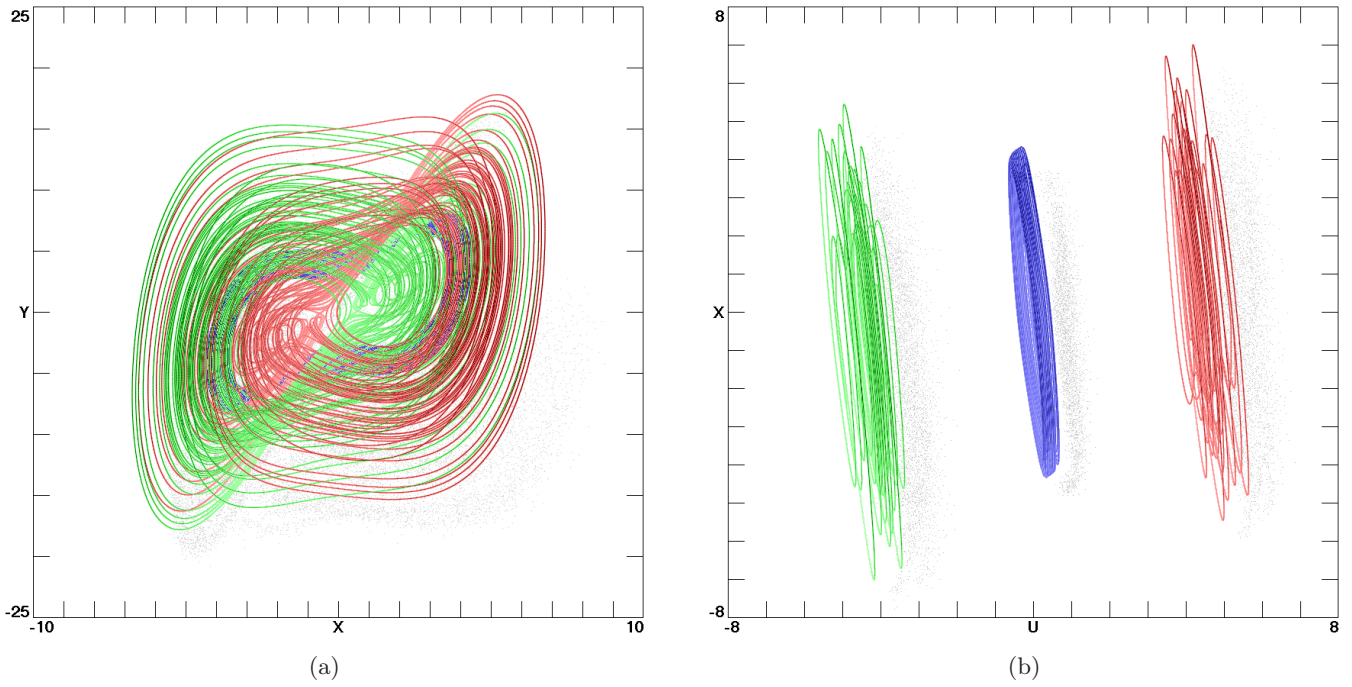(a)   (b)

Fig. 10. Torus with LEs $(0, 0, -0.1696, -0.8304)$ coexisting with a symmetric pair of strange attractors with LEs $(0.2520, 0, -0.0052, -1.2467)$ at $a = 6$, $b = 0.1$ (green and red attractors correspond to two symmetric initial conditions $(0, \pm 4, 0, \mp 5)$, and blue at initial conditions $(1, -1, 1, -1)$), (a) x–y plane and (b) u–x plane.
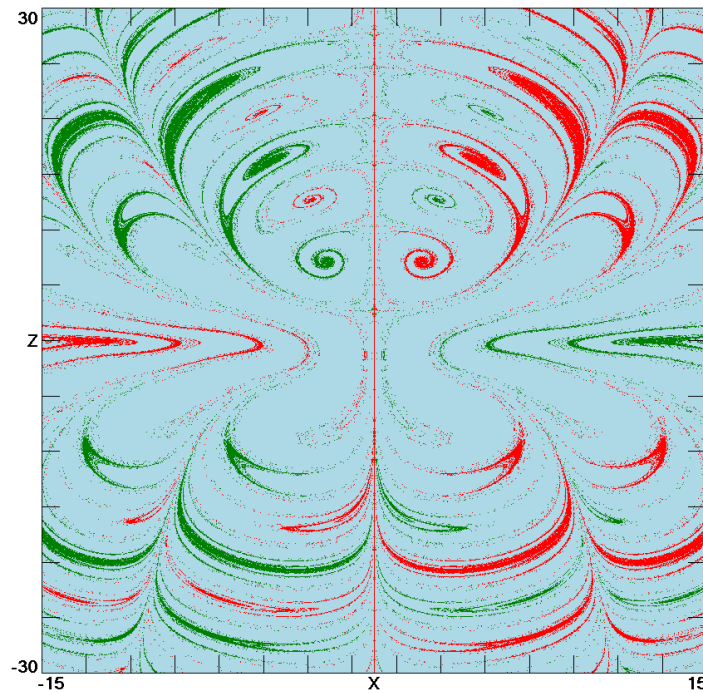

Fig. 11. Cross-section for $y = 0$ and $u = 0$ of the basins of attraction for the torus (blue) and the two strange attractors (red and green) of system (1) at $a = 6$, $b = 0.1$.
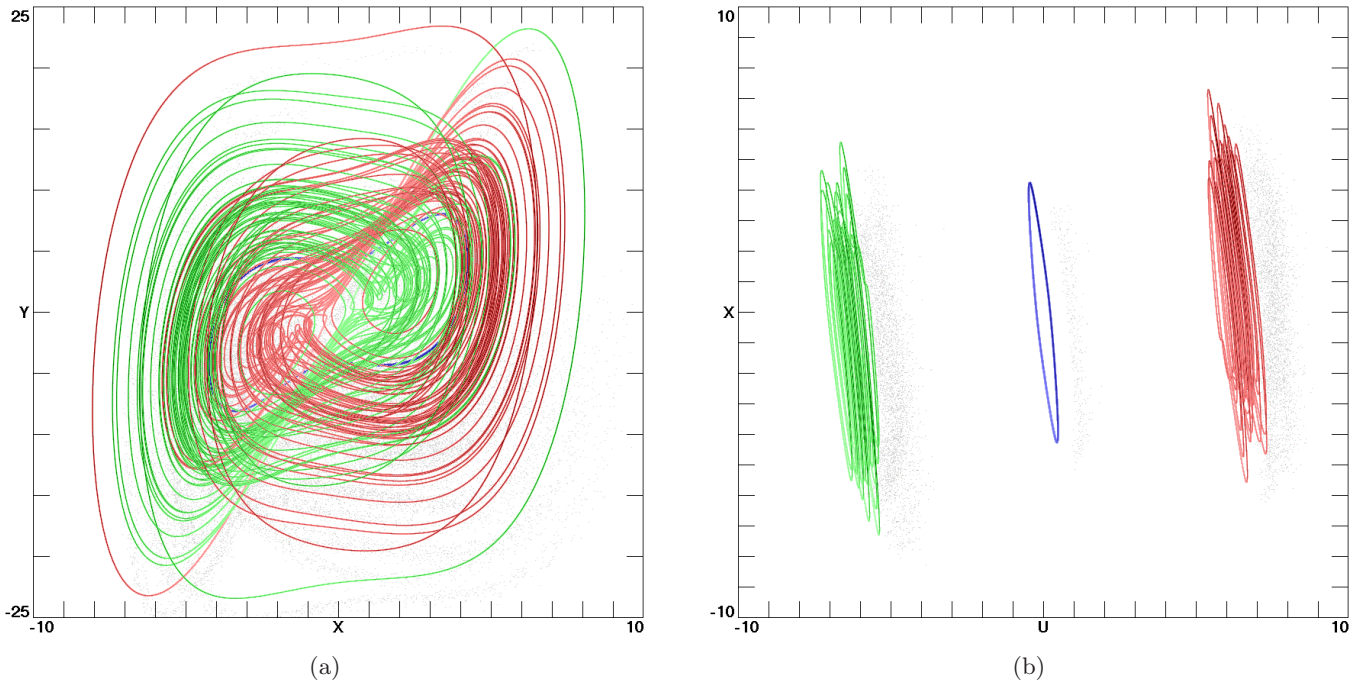
(a)

(b)

Fig. 12. Limit cycle with LEs $(0, -0.0227, -0.0227, -0.9547)$ coexisting with a symmetric pair of strange attractors with LEs $(0.2269, 0, -0.0102, -1.2167)$ at $a = 7$, $b = 0.1$ (green and red attractors correspond to two symmetric initial conditions $(0, \pm 7.8, 0, \mp 5)$ and blue at initial conditions $(1, -1, 1, -1)$), (a) x–y plane and (b) u–x plane.
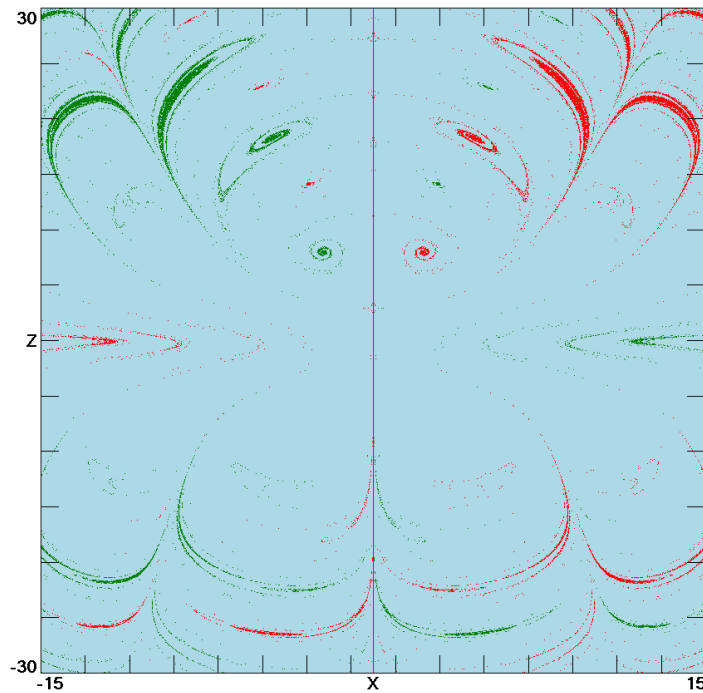

Fig. 13. Cross-section for $y = 0$ and $u = 0$ of the basins of attraction for the limit cycle (blue) and the two strange attractors (red and green) of system (1) at $a = 7$, $b = 0.1$.

6. Discussion and Conclusion

A relatively simple equilibrium-free system with only seven terms and two parameters that exhibits hyperchaos and coexisting hidden attractors has been described in this paper. A significant characteristic of this system is that it has a quasi-periodic torus over a large region of parameters. Furthermore, the torus coexists with either a symmetric pair of limit cycles or a symmetric pair of strange attractors over regions in parameter space, and a limit cycle coexists with two strange attractors in other regions. The dynamical regions are mapped, and fractal basin boundaries are observed, which show that the system is delicate with respect to both parameters and initial conditions.

We briefly examined a generalization of system (1) in which the quadratic nonlinearities are replaced by $x|z|^\gamma \text{sgn}(z)$ and $x|y|^\gamma \text{sgn}(y)$ in the second and third dimensions, respectively, and we find that when $\gamma = 3$, the corresponding system seems not to allow a torus, although it can be hyperchaotic.

Acknowledgments

References

Chlouverakis, K. E. & Sprott, J. C. [2006] "Chaotic hyperjerk systems," *Chaos Solit. Fract.* **28**, 739–746.

Gao, T., Chen, G., Chen, Z. & Cang, S. [2007] "The generation and circuit implementation of a new hyperchaos based upon Lorenz system," *Phys. Lett. A* **361**, 78–86.

Gao, Z. & Zhang, C. [2011] "A novel hyperchaotic system," *J. Jishou Univ.* (*Natural Science Edition*) **32**, 65–68.

Leonov, G. A. & Kuznetsov, N. V. [2013] "Hidden attractors in dynamical systems from hidden oscillations in Hilbert–Kolmogov, Aizerman, and Kalman problems to hidden chaotic attractors in Chua circuits," *Int. J. Bifurcation and Chaos* **23**, 1330002.

Li, Y., Chen, G. & Wallace, K. S. T. [2005] "Controlling a unified chaotic system to hyperchaotic," *IEEE Trans. Circuits Syst.-II*: *Exp. Briefs* **52**, 204–207.

Lorenz, E. N. [1963] "Deterministic nonperiodic flow," *J. Atmos. Sci.* **20**, 130–141.

Mirus, K. A. & Sprott, J. C. [1999] "Controlling chaos in low- and high-dimensional systems with periodic parametric perturbations," *Phys. Rev. E* **59**, 5313–5324.

Munmuangsaen, B. & Srisuchinwong, B. [2009] "A new five-term simple chaotic attractor," *Phys. Lett. A* **373**, 4038–4043.

Newhouse, S. E., Ruelle, D. & Takens, F. [1971] "Occurrence of strange axiom A attractors near quasi-periodic flows on T^m, $m \geq 3$," *Commun. Math. Phys.* **64**, 35–40.

Paar, V. & Pavin, N. [1998] "Intermingled fractal Arnold tongues," *Phys. Rev. E* **57**, 1544–1549.

Qi, G., Van Wyk, M. A., Van Wyk, B. J. & Chen, G. [2008] "On a new hyperchaotic system," *Phys. Lett. A* **372**, 124–136.

Rössler, O. E. [1979] "An equation for hyperchaos," *Phys. Lett. A* **71**, 155–157.

Ruelle, D. & Takens, F. [1971] "On the nature of turbulence," *Commun. Math. Phys.* **20**, 167–192.

Ruy, B. [2007] "Dynamics of a hyperchaotic Lorenz system," *Int. J. Bifurcation and Chaos* **17**, 4285–4294.

Si, G., Cao, H. & Zhang, Y. [2011] "A new four-dimensional hyperchaotic Lorenz system and its adaptive control," *Chin. Phys. B* **20**, 010509.

Sprott, J. C. & Rowlands, G. [2001] "Improved correlation dimension calculation," *Int. J. Bifurcation and Chaos* **11**, 1861–1880.

Sprott, J. C. [2007] "Maximally complex simple attractor," *Chaos* **17**, 033124.

van der Schrier, G. & Maas, L. R. M. [2000] "The diffusionless Lorenz equations: Shil'nikov bifurcations and reduction to an explicit map," *Phys. Nonlin. Phenom.* **141**, 19–36.

Wang, H., Cai, G., Miao, S. & Tian, L. [2010] "Nonlinear feedback control of a novel hyperchaotic system and its circuit implementation," *Chin. Phys. B* **19**, 030509.

Wang, Z., Cang, S., Ochola, E. O. & Sun, Y. [2012] "A hyperchaotic system without equilibrium," *Nonlin. Dyn.* **69**, 531–537.

Wolf, A., Swift, J. B., Swinney, H. L. & Vastano, J. A. [1985] "Determining Lyapunov exponents from a time series," *Physica D* **16**, 285–317.